ICAS-98-5,4,5

EXPERIEMENTAL INVESTIGATION OF AXIAL COMPRESSOR CASCADE PERFORMANCE UNDER THE INFLUIENCE OF LOW INTENSITY TURBULENCE

J. K. Mukhraiya and N. A Ahmed

A98-31638

School of Mechanical and Manufacturing Engineering
The University of New South Wales
SYDNEY 2052 Australia

ABSTRACT

The performance of an axial compressor cascade is greatly affected by free stream turbulence level, mainly due to its influence on the transition from laminar to turbulence boundary layer, its development and any subsequent separation. The present investigation describes the effects of low level turbulence intensity on the performance of an axial compressor cascade. A C-4 profile cascade was placed at the exit of a blow-down wind tunnel. The turbulence level was varied from 0.91% to 5.97 % using a turbulence generating grid upstream of the cascade. The Reynolds Number was below the critical range (0.80×10^5 to 0.87×10^5). The results show that the effects of upstream turbulence level on the cascade are significant and the effects of Reynolds Number and turbulence level are interrelated.

INTRUDUCTION

Axial compressor cascade performance has been studied extensively under the influence of various design and operating parameters (1-9). Evan (2) investigated the influence of turbulence level on the turbulent boundary layer in a compressor cascade and found that the variations in turbulence level does affect the behavior of the laminar and turbulent boundary layers. Its main local effects are on transition and the laminar separation bubble. The effect of Reynolds Number in the cross over range ($10^5 < 10^6$) tends to be less predictable and the changes in the critical range are relatively abrupt, once the boundary layer separation takes place. Horlock et al (10) concluded that the performance below the critical point is unpredictable, but the effects of Reynolds Number are not. Thus the overall correlation for the effect of turbulence level on blade performance becomes unreliable. Masek and Norbury (11) showed that with higher main stream turbulence level, the suction surface boundary layer undergoes a nearly normal transition with some indication of a small bubble, while at the lower turbulence level there is a marked laminar separation bubble at mid chord. They further showed that at incidence below the design value, the effect of increasing axial velocity ratio on the boundary layer development was comparatively small so that there were only small changes in the deviation and loss coefficient. Schlichting and Das (12) studied the cascade flow problem and concluded that the critical turbulence level does exist under adverse pressure gradient conditions. Gostelow (13) also indicated a critical turbulence level. Shaw (14) determined the overall performance of an isolated rotor at different Reynolds Number and turbulence level. He concluded that the variation in the turbulence intensity varies with the axial velocity in the compressor. Pollard and Gostelow (3) suggested the if porous side walls were used to control the side wall boundary layer a low aspect ratio cascade would give two-dimensional results. Further more a high level of free stream turbulence tends to promote early boundary layer transition and hence delays the increase in the losses, normally associated with Reynolds Number.

Since Reynolds Number and turbulence level effects are closely related, it has been suggested (13) that the concept of an effective Reynolds Number may be used to correlate the various

21st ICAS Congress
13-18 September 1998
Melbourne, Australia

degrees of turbulence levels and Reynolds Number. However, Martlew (14) has disagreed with this approach and observed that the relationship is not linear He found that, as the turbulence level was raised from 0.18% to 1.5% the separation point moved rearward. Further increases in turbulence level up to 3% had little or no effects. So, he concluded that though the Reynolds Number and turbulence level are closely related, they should be treated as separate experimental variables.

In the present work, the effects of low intensity turbulence level on axial compressor cascade performance are investigated. The tests were conducted at the turbomachinery Laboratory of IIT Delhi.

NOMENCLATURE

C	= Absolute Velocity
C_x	= Axial Velocity
l	= Chord Length
P	= Static Pressure
μ	= absolute viscosity
x, y	= Coordinate
a	= Maximum camber from leading edge
s	= pitch of the blade
α	= Flow angle
α'	= Blade angle
C_m	= Mean velocity
i	= Incidence angle
δ	= Deviation angle
λ	= Stagger angle
θ	= Camber angle
ε	= Deflection angle
ρ	= Air density
AVR	=Axial Velocity Ratio $= C_2 \text{Cos } \alpha_2 \ / C_1 \text{Cos } \alpha_1$
C_D	=Coefficient of drag $= \xi(s .\text{Cos}^2 \alpha_m / l \text{Cos}^2 \alpha_1)$
C_L	=Coefficient of lift $= s/l \text{ Cos } \alpha_m(\text{Tan } \alpha_1 - \text{Tan } \alpha_2) - C_D \text{ Tan } \alpha_m$
C_P	= Static Pressure Coefficient $= P_2 - P_1 / (\frac{1}{2} C^2 \rho)$
α_m	= Mean Flow Angle $= \text{Tan}^{-1(\text{Tan } \alpha 1 + \text{Tan } \alpha 2)} / 2$
ξ	= Stagnation Pressure Loss Coefficient $= (P_{01} - P_{02}) / (\frac{1}{2} C^2 \rho)$
Re	= Reynolds Number $= C_1 \rho l / \mu$

SUBSCRIPT

0	=Stagnation condition
1	=Upstream of the cascade
2	=Down Stream of the cascade

EXPERIMENT

A. SETUP

The experimental setup consists of an air supply unit, a wind tunnel, turbulence generating grid, a constant temperature hot wire anemometer system, cascade of axial compressor blades (as per the NASA report No. 1016) and a multitude water column manometer to measure pressure at different locations. The test rig arrangement is shown in fig. 1. Air was supplied to the test section using a backward swept centrifugal blower, which was coupled with a 25 kW variable speed D.C. motor having a speed range of 0-3000 RPM. The wind tunnel, used in the present investigation was an open circuit low speed wind tunnel. The cross section of the settling chamber was 1220 mm x 1220 mm and the working section was 305 mm x 305 mm. The turbulence generating cross section was reduced to a size of 205 mm x 305 mm at the inlet of the cascade in order to accommodate the turbulence generating grid. To visualise the position of the grid one of the walls of the section was made-up of Perspex sheet. The grid was made up of wooden rods of 6.5 mm diameter. To vary the turbulence level, the geometry of this grid was altered by changing the number of rods. A three-hole pressure probe was used for measuring the stagnation pressure, static pressure, velocity and the direction of flow. The magnitude of pressure was recorded in terms of water gauge using an inclined water column manometer. The pressure probe consisted of three hypodermic stainless steel tubes of 0.9mm diameter O.D. A simple traversing mechanism was developed for accurate traversing of the probe in axial and circular direction. The probe along with the traversing mechanism was mounted on a specially developed steel frame. The probe was calibrated for dynamic head against a standard NPL Pitot-static tube in the test section of the wind tunnel. The probe was also calibrated for the angle error and connected to the manometer through Tygon tubes. The static pressure at various locations was recorded with the help of static pressure taping with an orifice diameter of 0.8 mm. These tapings were fixed perpendicular to the direction of flow and were flush mounted with the surface of the wall and connected to the manometer.

The turbulence intensity upstream of the cascade was measured with using a Southampton make constant temperature hot wire anemometer system (20 IB ISVR). It consisted of a builtin linearisation circuit to provide linear calibration for the probe. A hot wire probe was fabricated as per the directions given in the manual and it was calibrated against a standard NPL pitot-static probe in the

test section of the wind tunnel regularly. The cascade blades used in this investigation, have a C-4 profile with a chord of 89 mm and a pitch of 80 mm. The blades were 200 mm in height, has a camber of 30^0 and were fixed at 45^0. This configuration gives an aspect ration of 2.25 and stagger angle of 45^0. A total number of seven blades were used in the cascade to give good periodicity at subsonic speed (13). On the central blade surface seventeen hypodermic tubes of 19 SWG were buried to form the central instrumented blade. A hole of 05 mm was drilled through all the tubes at the mid span position (Fig.1B) which were than connected to the water column manometer to obtain the static blade surface pressure distribution.

The axial velocity ratio (AVR) and aspect ratio of a cascade are important parameters in affecting the stall point. It has been suggested (16) that the increase in AVR due to side wall boundary layer, invalidate most results and an aspect ratio below two should not be used. Therefore in the present study, the cascade was provided with porous side walls, with out any side wall suction arrangement and an aspect ration of 2.25 was used.

B PROCEDURE

In this study of cascade performance, measurements of various parameters were made. The total pressure upstream of the cascade was measured using the three-hole pressure probe, placed at a distance of one chord from the blade leading edge. The probe was mounted on the frame, which was attached with one of the side walls. The probe was traversed from one side wall to the other wall of the cascade (perpendicular to the cascade wall) and also parallels to the wall covering a distance of seven blade pitch. An attachment, similar to the upstream side was also provided down stream side of the cascade. The traversing was also performed at one chord distance down stream. The down stream traversing was performed only at mid span position parallel to the cascade walls, since the function of down stream traversing was merely to record the cascade effects on the entry flow.

The turbulence generating grid was placed across the entrance to the wind tunnel working section at a distance, equal to ten-blade pitch from the cascade centre. The geometry of the grid was changed in such a manner that its uniformity could be maintained to produce near isotropic turbulence. A hot wire probe was traversed upstream of the cascade at a distance of five blade pitch. The probe, was mounted on a specially designed traversing attachment, fixed in the test section of the wind tunnel. D.C. and A.C. RMS components of the fluctuating velocity were recorded with the help of a D.C. voltmeter and an A.C RMS voltmeter, connected to the anemometer. The turbulence intensity was determined using the relationship obtained from reference (17)

A series of experiments were conducted to investigate the effect of upstream flow conditions. The upstream turbulence intensity was varied in the rang of 0.91% with the help of a turbulence generating grid. The incidence angle was varied from -15^0 to $+30^0$ by adjusting the turntable of the cascade. The Reynolds Number variations were in the range of 0.80×10^5 to 0.87×10^5. Preliminary tests were carried out to assess the cascade performance in the absence of grid. Detailed experiments were performed using different grid geometry combinations in order to vary the turbulence level. Records of static pressure and dynamic pressure before and after the cascade were obtained for different values of Reynolds Number, turbulence intensity and incidence angle. In addition, static pressure at different points on the blade surface was also recorded. These experiments were repeated for a number of grid geometry combinations. The experimental data were processed on an IBM compatible and turbulence intensity, static pressure coefficient, stagnation pressure loss coefficient, Reynolds Number and lift coefficient and drag coefficient were obtained. The results are presented graphically as the variation of stagnation pressure loss coefficient, static pressure coefficient, lift coefficient and drag coefficient with incidence angle. The experimental results have some uncertainty due to the inaccuracies involved in the measured quantities. The uncertainties in total pressure loss coefficient, drag coefficient, Lift coefficient and turbulence level were calculated as per the reference (18) and were found to be 0. 83%, 1.16%, 1.67% and 2.44% respectively

DISCUSSION OF RESULTS

The variations of inlet flow profile at different levels of turbulence is shown in fig. 1(D). It indicates almost uniform flow pattern over the five blade passages and practically no change in the flow pattern with different turbulence levels. Some preliminary tests were carried out without turbulence generating grid. For this set of experiments Reynolds Number and turbulence intensity up stream of the cascade were measured as 0.91×10^5 and 0.9%. The variation of lift and drag coefficient is shown in fig.2. In all these cases it is observed that the lift coefficient increases with an increase in the angle of incidence up to +5%. Further increase in the value of incidence angle, reduces the lift

coefficient drastically due to blade stall. The drag coefficient decreases slightly with an increase in the incidence and remains almost constant up to +5% incidence and thereafter it increases suddenly. The effect of turbulence intensity on the lift and drag coefficient is significant. With an increase in turbulence level up to 2.8%, lift coefficient increases considerably and in consequences drag coefficient decreases. This indicates that the small increase in turbulence level is favorable in delaying the separation of flow from blade surface and thereby increases the lift coefficient. Further more at a higher value of Reynolds Number (0.86×10^5) an increase in drag coefficient indicates a low efficiency of diffusion through the blade passage. Fig.3 shows the similar variations for lift and drag coefficient for different values of turbulence level. From the above discussion it is clear that although the values of lift and drag coefficient varies significantly with the variation of turbulence intensity, an accurate quantification of effect of turbulence level on lift and drag forces is still difficult.

The most important factor for blading is its loss coefficient. The variation of stagnation pressure loss coefficient with the angle of incidence is given in fig. 4. The stagnation pressure loss coefficient is highest at a turbulence intensity of 3.82 % and is lowest at a value of 5.47 %. This variation in stagnation pressure loss coefficient is similar to the variation of drag coefficient and the effects of turbulence level are unpredictable. It is observed that the stagnation pressure loss coefficient is slightly higher at a negative incidence (-10^0), but when the incidence angle is varied towards the positive side, the value of loss coefficient falls up to $+5^0$. With further increase in the value of incidence angle, the stagnation pressure loss coefficient increases sharply. This nature of loss coefficient is expected, since the drag coefficient is a function of stagnation pressure loss coefficient. The increase in total pressure loss coefficient is significant as the angle of attack increased beyond a value of $+5^0$. In this case it is difficult to define the precise incidence at which stalling occurred, but it can be roughly estimated as the incidence at which mean total pressure loss in the stalled region is increased by 50 %. Viscous effects reduces the velocity of flow adjacent to the surface of the cascade with subsequent rise in stagnation pressure loss coefficient and coefficient of drag with an increase in the value of Reynolds Number. Further a high value of loss coefficient (0.2-0.4) has been observed from the plot. This may be assigned to the overall low value of Reynolds Number. On the basis of composite plots of loss coefficient for cascade as a function of Reynolds Number, it has been observed that as the Reynolds Number was reduced to a critical value between 0.5 to 2 $\times 10^5$, the losses rises abruptly (19) Some studies on the critical nature of reduction in Reynolds Number below 2×10^5have been reported in the literature. It has been noticed that, the critical Reynolds Number reduced to half by the instructions of turbulence. An increase in turbulence level has similar effect on the boundary layer development. Both the factors contribute to a high rate of momentum exchange between boundary layer and free stream and thus produce higher losses (20), Shaw (15) also concluded that when the Reynolds Number was reduced below the critical limit, a sharp increase in the losses occurred. Fig. 5 presents the variation of deflection angle with incidence. It is noted that the value of deflection angle increases continuously as the value of incidence increased from -10^0 to about $+10^0$. Further increase in the incidence causes deflection angle to fall rapidly. It is also noted that the peaks of all the curves shifted towards higher values of incidence angle with reduction in turbulence level of 3.12% and the lowest value was obtained at 5.47%. At approximately $+5^0$ incidence, all the curves come closer, indicating an optimum value of incidence. Thus the figure displayed an erratic behavior of turbulence level variation with deflection angle. The variation of static pressure coefficient against the angle of incidence is presented in fig. 6. The values of static pressure coefficient for all the levels of turbulence are higher at -10^0 of incidence, and it decreases with an increase in the incidence angle towards positive side. At 0^0 incidence the value of static pressure coefficient is the lowest in all the cases. With further increase in the values of incidence, the pressure coefficient increases sharply (up to a value of $+20^0$) and then decreases again with increases in the incidence. The highest value of pressure coefficient occurs at 0^0 incidence with a turbulence level of 3.82% and 20^0 incidence, it is the highest with a turbulence level of 3.12%.

The effect of turbulence level variations on the static pressure coefficient across the cascade is much smaller at negative incidence, since the flow was almost two-dimensional. The axial velocity variations had little effect on the boundary layer development, so only small changes in the pressure coefficient were observed at incidence below the design value. At the higher value of positive incidence boundary layer growth on the blade surface would affect the axial velocity variations, resulting in large variations in the static pressure coefficient. This characteristic of static pressure coefficient demonstrate the importance of turbulence level and its arbitrary nature.

The variation of blade static pressure coefficient with the blade chord are presented through fig 7 to 10. Fig. 7 shows the variation at an incidence of $+5^0$. It is shown that as the turbulence intensity increase a separation bubble seems to appear on the suction surface, about 70% of the chord length from the leading edge. Further more the value of pressure coefficient is smaller for higher values of turbulence level and a high-pressure zone near the trailing on the pressure surface is also observed. At 0^0 incidence (Fig. 8), the characteristics of the static pressure coefficient are similar to the above case, but in this case the value of pressure coefficient is lower and separation bubble seems to have appeared on suction side at 20% chord length. At lower turbulence level there is a marked laminar separation. This gives a greater boundary layer growth down stream of the blade, leading to the larger wakes. At higher values of turbulence level (fig 9-10), the nature of pressure coefficient curve is similar to the earlier case. With the higher main stream turbulence the suction surface boundary layer undergoes a nearly normal transition. This suggests that the radial movement of the blade surface boundary layer have a significant effect on the variation of static pressure coefficient. Further the separation bubble becomes more pronounced at low values of Reynolds Number. This separation of flow between the wall and the blade suction surface modified the angle distribution and thus increases losses. These secondary losses occurred in the cascade, may be associated with larger losses and with separation near the side walls. The variation of static pressure coefficient at different values of incidence and turbulence level are shown in fig. 11-12. In almost all the cases it is observed that the value of pressure coefficient is higher at a value of incidence at $+5^0$. At 0^0 incidence it is very close to the values obtained at $+5^0$ incidence. Also at negative incidence (-5^0), the pressure coefficient is almost on the negative pressure side. This suggests that at -5^0 incidence the blade is entirely stalled. As the level of turbulence increases a separation bubble on the suction side surface began to appear about 70 % of the chord. Some kinks on the blade surface are also observed. This could be the interaction of end wall boundary layer with the cascade, which causes them to turn perpendicularly on the pressure surface and may results in an irregular pressure distribution. Also a major portion of losses produced in the cascade are associated with the transition separation on the blade surface. The boundary layer is less able to withstand, an adverse pressure gradient and unable to reattach itself as a turbulent boundary layer.

CONCLUSIONS

From the results reported in this experimental study, following conclusions may be drawn

1. As the turbulence level increases the stagnation pressure loss coefficient increases slightly in the lower range of incidence, but in the higher range of incidence, the stagnation pressure loss coefficient decreases with increases in turbulence intensity.

2. The values of deflection angle vary abruptly with increase in turbulence intensity. The peak value of deflection occurs at higher positive value of incidence.

3. As the incidence is increased beyond +5%, drag coefficient increases and in consequence lift coefficient decreases. Further the Reynolds Number effects are not significant at low value of turbulence level

4. The static pressure coefficient is higher at negative values of incidence, but as the incidence is increased, the static pressure coefficient reached to its peak and than decreases with further increase in the value of incidence. The effaces of turbulence level on pressure coefficient are arbitrary.

5. As the incidence decrease, the blade surface pressure coefficient also decreases. Further the turbulence level variations have considerable effects on the blade surface static pressure distribution.

REFERENCE

1. Abu-Ghannam and Shaw, R. Natural Transition of Boundary Layers: The Effects of Turbulence, Pressure gradient and Flow History". J. Mech. Eng. Science (1980)

2. Evans R.L. "Streams Turbulence effects on the Turbulent Boundary Layer in a Compressor Cascade". ARC No.34587, 1973.

3. Pollard D. and Gostelow J.P. "Some Experiments at Low Speed on Compressor cascade" Trans. ASME J. of Eng. Power 1967.

4. Potter J.L. Barnett, R.J. Koukousakis, C.E. and Fisher, C.E. "Detachment of Turbulent Boundary Layer With Varying Free Stream Turbulence and Low Reynolds Number" Proc. Conf. on Low Reynolds Number Aerodynamics, Norte Damr Indiana USA, 5-7 June 1989.

5. Kestoras M.D. and Simon T.W. "Effects of Free stream Turbulence Intensity on a Boundary Layer Recovering from Concave Curvature Effects" Trans. ASME J. of Turbomachinery 1995 Vol. 117

6. Kang, S. and Hirch, C. "Experimental Study on the Three Dimensional Flow Within a Compressor Cascade With Tip Clearance: Part-I Velocity and Pressure Fields Part II The Tip Leakage Vortex Trans. ASME J. of Turbomachiner July 1993 Vol. 115

7. Roberts W.B. "The Effect of Reynolds Number and Laminar Separation on Axial Cascade Performance" Trans. ASME J. of Eng. For Power. 1975

8. Yocum, A.M. O'Brien W.F. "Separated Flow in a Low-Speed Two Dimensional Cascade: Part-I Flow Visualization and Time Mean Velocity Measurements, Part – II Cascade Performance Trans. ASME J. of Turbomachinery July 1993 Vol. 115.

9. Gostelow J.P., Bluden A.R. and Walker G.J. " Effects of Free Stream Turbulence and Adverse Pressure Gradients on Boundary Layer Transition" Trans. ASME J. of Turbomachinery July 1994 Vol. 116

10. Horlock, J.H. , Shaw R., Pollard, D. and Lew Kowicz A. "Reynolds Number effects in Cascade and Axial Flow Compressor" Trans. ASME J. Mech. Eng. Power July 1964

11. Masek, Z. and Norbury, J.F. "Low Speed Performance of a Compressor Cascade Designed for Prescribed Velocity Distribution and Tested with Axial Velocity Ratio" Proc. Inst. Mech. Engrs. Conference 1973

12. Schlichting, H. and Das, A. "Recent Research on Cascade Flow Problems". Trans. ASME J. of Basic Eng. 1966

13. Gostelow J.P. "Cascade Aerodynamics" Pergamon Press Ltd. 1984

14. Martlew, D.L. "Measurement of the Performance of a Cascade of Compressor Blade under Various Degrees of Intensity of Turbulence in the Air stream" ARC Report No. 15 1982

15. Shaw, R. "The effect of Reynolds Number, Turbulence Intensity and Axial Velocity Ratio on Compressor Blade Performance" Proc. Inst. Mech. Engrs. 1969-70

16. Ilays, M. and Norbury, J.F. "Effect of Axial Velocity Variations on the Subsonic Flow through a Compressor Cascade". I Mech. Eng. Conference Publication, 1973

17. Hoole, B.J. and Calvert, J.R. "The use of Hot Wire Anemometer in Turbulent Flow" J. Royal Aero Society Vol. 71- July 1967

18. Moffat, R. J. "Using Uncertainty Analysis in the Planning of an Experiment" Trans. ASME J. of Eng. For Power 1967

19. "Aerodynamic Design of Axial Flow Compressor" NASA SP –36, 1965

20. Blight, F.G. and Howard, W. "Test on Four Aerofoil Cascades Part –I "Deflection, Drag and Velocity Distribution" Part-II "Boundary Layer Characteristics" Resp. E-74 and E-75 ARL Australia 1952.

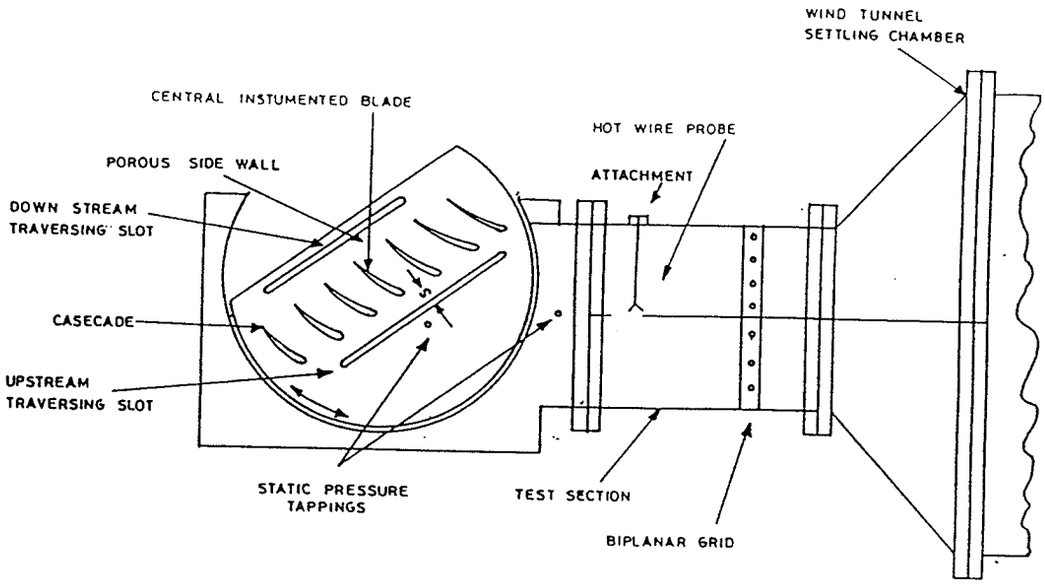

FIG. 1 (A) TEST RIG

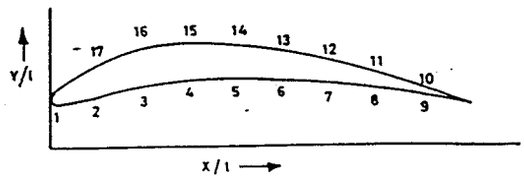

FIG. 1 (B) COORDINATE OF PRESSURE HOLE

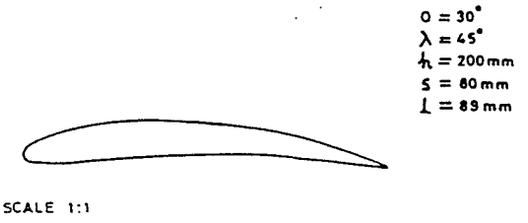

FIG 1(C) COORDINATES & C-4 PROFILE BLADE

No. OF PRESSURE HOLE	1	2	3	4	5	6	7	8	9
		17	16	15	14	13	12	11	10
DISTANCE FROM LEADING EDGE mm	00	10	20	30	40	50	60	70	80

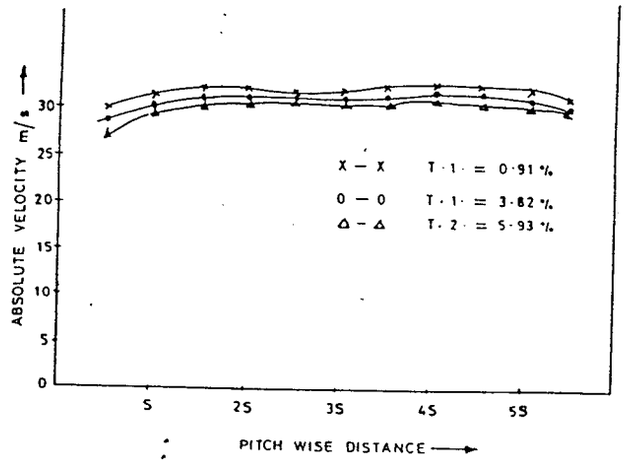

FIG. 1 (D) UPSTREAM VELOCITY PROFILE

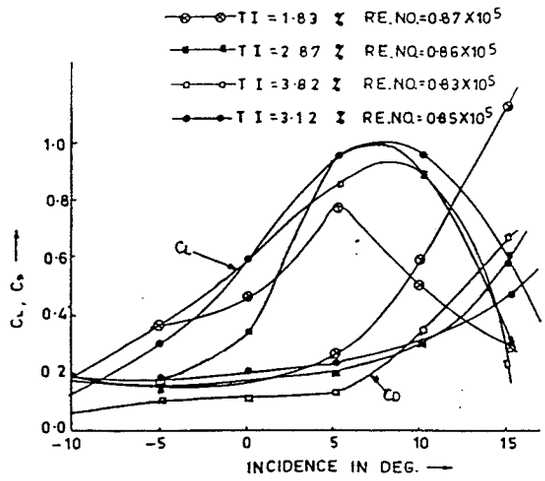

FIG. 2 VARIATION OF LIFT AND DRAG COEFFICIENTS WITH INCIDENCE.

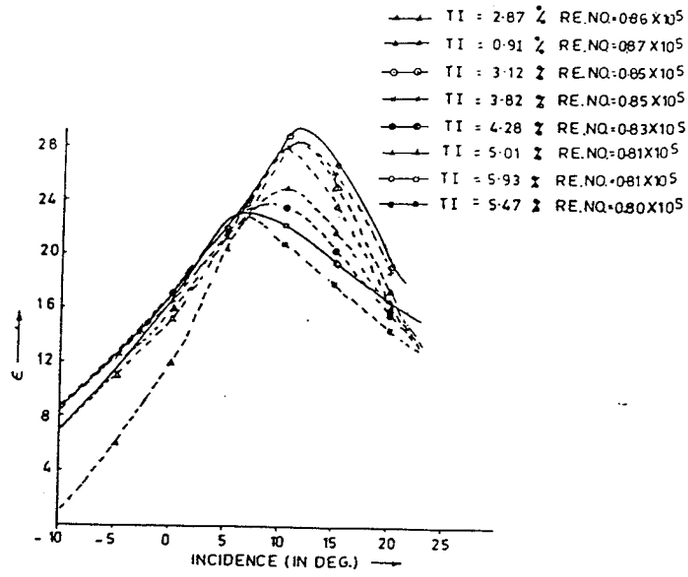

FIG.5 VARIATION OF DEFLECTION ANGLE WITH INCIDENCE.

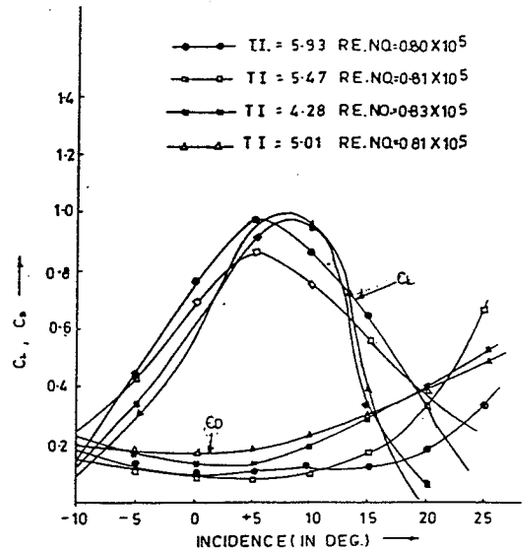

FIG. 3 VARIATION OF LIFT AND DRAG COEFFICIENTS WITH INCIDENCE.

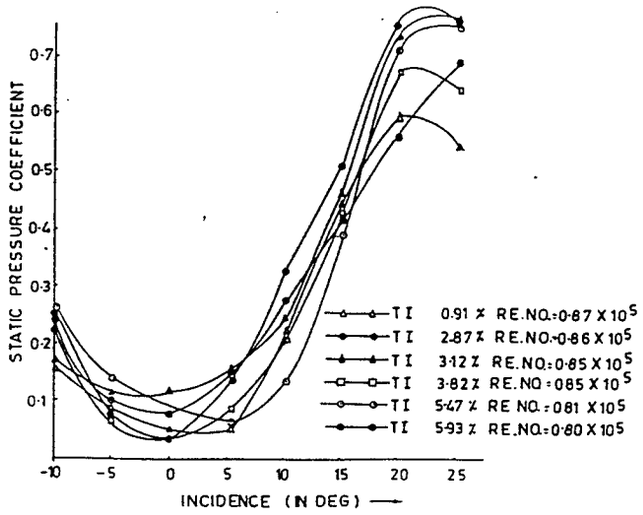

FIG.6 VARIATION OF STATIC PRESSURE COEFFICIENT WITH INCIDENCE.

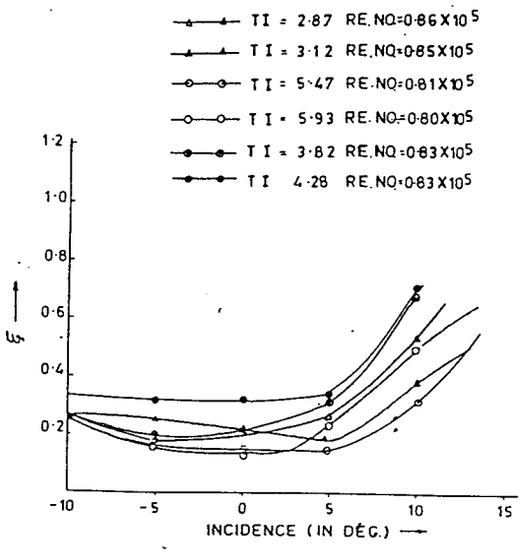

FIG. 4 VARIATION OF STAGNATION PRESSURE LOSS. COEFFICIENT WITH INCIDENCE.

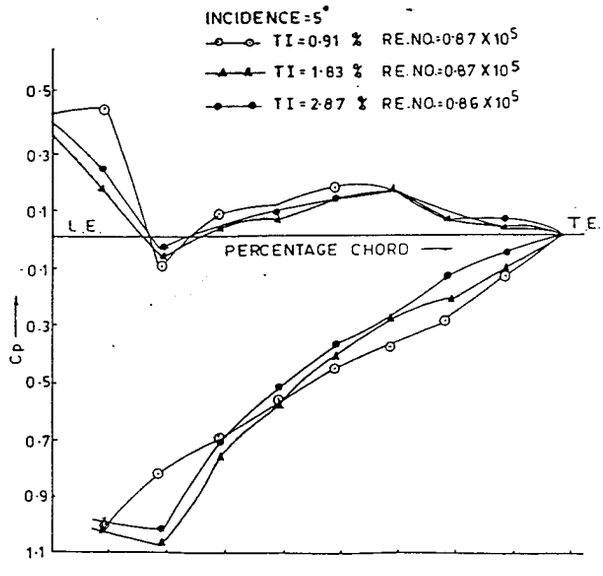

FIG.7 BLADE LOADING DIAGRAMS AT 5° INCIDENCE.

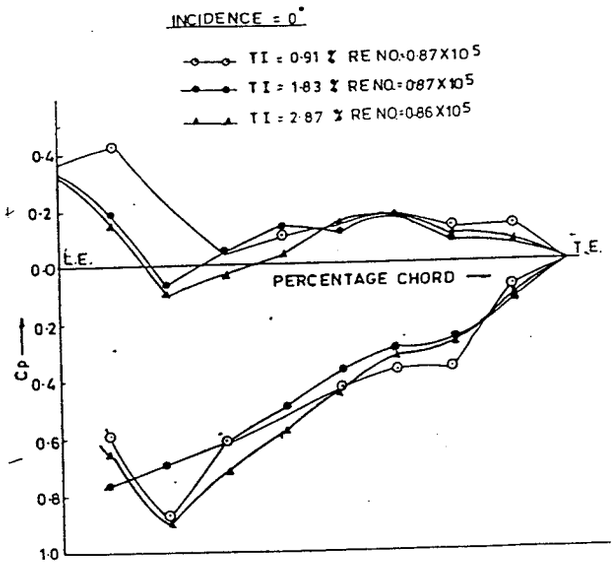

FIG.8 BLADE LOADING DIAGRAMS AT 0° INCIDENCE

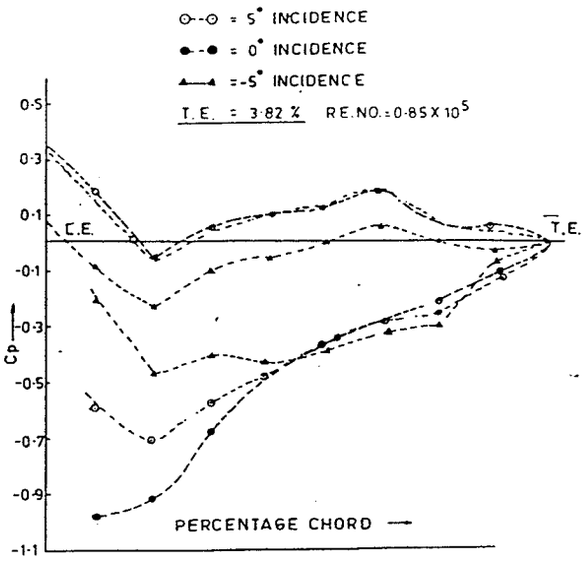

Fig 11 BLADE LOADING DIAGRAM AT DIFFEREN ANGLE OF INCIDENCE.

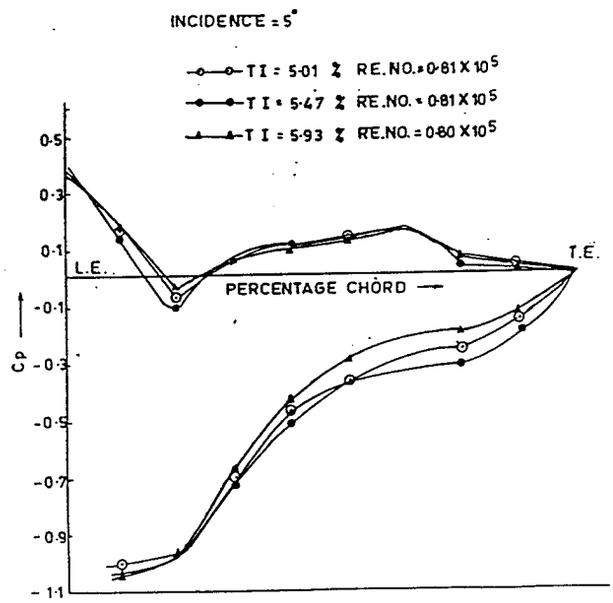

FIG.9 BLADE LOADING DIAGRAMS AT 5° INCIDENCE.

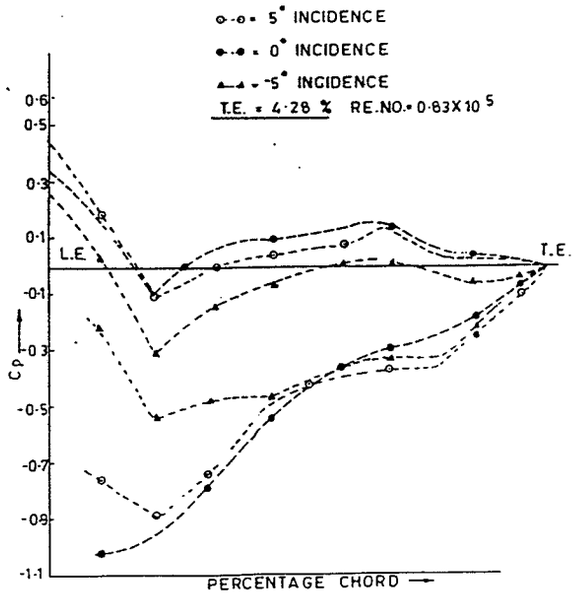

Fig12 BLADE LOADING DIAGRAM AT DIFFERENT ANGLE OF INCIDENCE

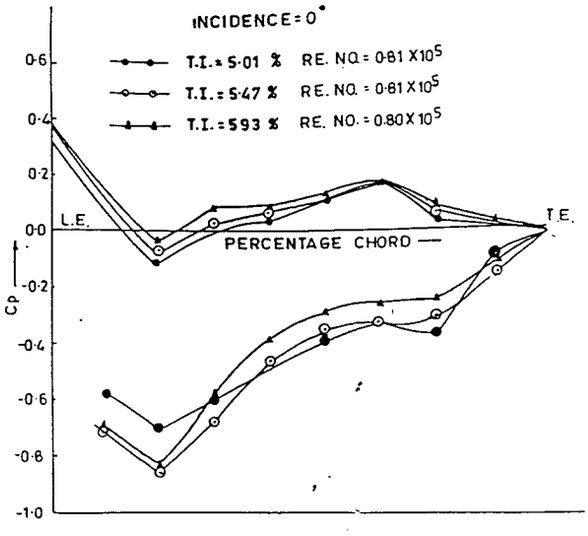

FIG.10 BLADE LOADING DIAGRAM AT 0° INCIDENCE